

2004

# Facet joint kinematics and injury mechanisms during simulated whiplash

Adam MacKay Pearson  
*Yale University*

Follow this and additional works at: <http://elischolar.library.yale.edu/ymtdl>

---

## Recommended Citation

Pearson, Adam MacKay, "Facet joint kinematics and injury mechanisms during simulated whiplash" (2004). *Yale Medicine Thesis Digital Library*. 3023.  
<http://elischolar.library.yale.edu/ymtdl/3023>

This Open Access Thesis is brought to you for free and open access by the School of Medicine at EliScholar – A Digital Platform for Scholarly Publishing at Yale. It has been accepted for inclusion in Yale Medicine Thesis Digital Library by an authorized administrator of EliScholar – A Digital Platform for Scholarly Publishing at Yale. For more information, please contact [elischolar@yale.edu](mailto:elischolar@yale.edu).

MED  
T113  
+Y12  
7139

YALE UNIVERSITY LIBRARY



39002010657139

NECK JOINT KINEMATICS AND INJURY  
MECHANISMS DURING SIMULATED WHIPLASH

Adam MacKay Boarson

YALE UNIVERSITY

2004

YALE  
UNIVERSITY



CUSHING/WHITNEY  
MEDICAL LIBRARY

Adam Pearson


Permission to photocopy or microfilm processing of this thesis for the purpose of individual scholarly consultation or reference is hereby granted by the author. This permission is not to be interpreted as affecting publication of this work or otherwise placing it in the public domain, and the author reserves all rights of ownership guaranteed under common law protection of unpublished manuscripts.



Signature of Author

3/1/04

Date



Digitized by the Internet Archive  
in 2017 with funding from  
The National Endowment for the Humanities and the Arcadia Fund

<https://archive.org/details/facetjointkinema00pear>





**FACET JOINT KINEMATICS AND INJURY  
MECHANISMS DURING SIMULATED WHIPLASH**

A Thesis Submitted to the  
Yale University School of Medicine  
in Partial Fulfillment of the Requirements for the  
Degree of Doctor of Medicine

by

Adam MacKay Pearson

2004



T 113

+ Y 12

7139

## ABSTRACT

**FACET JOINT KINEMATICS AND INJURY MECHANISMS DURING SIMULATED WHIPLASH.** Adam M. Pearson, Paul C. Ivancic, Shigeki Ito, and Manohar M. Panjabi. Biomechanics Laboratory, Department of Orthopaedics and Rehabilitation, Yale University School of Medicine, New Haven, CT.

Clinical studies have implicated the facet joint (FJ) as a source of chronic neck pain in whiplash patients. Prior in vivo and in vitro biomechanical studies have evaluated FJ compression and excessive capsular ligament (CL) strain as potential injury mechanisms. No study has comprehensively evaluated FJ compression, FJ sliding and CL strain at all cervical levels during multiple whiplash simulation accelerations. The goal of this study was to describe FJ kinematics, including FJ compression and FJ sliding, and quantify peak CL strain during simulated whiplash. The whole cervical spine model with muscle force replication and a bench-top trauma sled were used in an incremental trauma protocol to simulate whiplash of increasing severity. Peak FJ compression (displacement of the upper facet surface towards the lower facet surface), FJ sliding (displacement of the upper facet surface along the lower facet surface) and CL strains were calculated and compared to the physiologic levels determined during intact flexibility testing. Peak FJ compression was greatest at C4-C5, reaching a maximum of 2.6 mm during the 5 g simulation. Increases over physiologic levels ( $p < 0.05$ ) were initially observed during the 3.5 g simulation. In general, peak FJ sliding and CL strains were largest in the lower cervical spine and increased with impact acceleration. CL strain reached a maximum of 39.9% at C6-C7 during the 8 g simulation. Facet joint components may be at risk for injury due to FJ compression during rear-impact accelerations of 3.5 g and above. Capsular ligaments are at risk for injury at higher accelerations.



## ACKNOWLEDGEMENTS

I would like to thank the following people: Dr. Manohar Panjabi for being the best mentor a student could ask for, Paul Ivancic for his patient teaching of someone unfamiliar with engineering, Shigeki Ito for his unique surgical insight, Wolfgang Rubin for his good-natured assistance with technical problems, my family for helping me get to this point, and Holly for her love and support.

This research was supported by NIH Grant 1 R01 AR45452 1A2 and the Doris Duke Charitable Foundation.



**TABLE OF CONTENTS**

<b>ABSTRACT.....</b>	<b>ii</b>
<b>ACKNOWLEDGEMENTS.....</b>	<b>iii</b>
<b>TABLE OF CONTENTS.....</b>	<b>iv</b>
<b>INTRODUCTION.....</b>	<b>1</b>
<b>STATEMENT OF PURPOSE.....</b>	<b>4</b>
<b>METHODS.....</b>	<b>5</b>
The Role of Various Investigators.....	5
Specimen Preparation and Radiography.....	5
Physiologic Facet Joint Displacements and Capsular Ligament Strains.....	8
Whiplash Simulation and Monitoring.....	9
Facet Joint Displacements and Capsular Ligament Strains During Whiplash.....	9
Error Analysis.....	10
Data Analysis.....	11
<b>RESULTS.....</b>	<b>13</b>
Representative Example.....	13
Six Specimens.....	14
<b>DISCUSSION.....</b>	<b>22</b>
<b>REFERENCES.....</b>	<b>27</b>



## INTRODUCTION

Though whiplash is a relatively common injury and results in significant costs to society, the underlying pathophysiology is poorly understood. Spitzer et al have defined whiplash as follows<sup>1</sup>:

"Whiplash is an acceleration-deceleration mechanism of energy transfer to the neck. It may result from rear-end or side-impact motor vehicle collisions, but can also occur during diving or other mishaps. The impact may result in bony or soft-tissue injuries (whiplash injury), which in turn may lead to a variety of clinical manifestations (Whiplash-Associated Disorders)."

Whiplash-associated disorders have a prevalence of 1% in the United States and cost an estimated 10 billion Euros per year in Western Europe.<sup>2,3</sup> Despite clinical and biomechanical research efforts, the underlying mechanisms causing whiplash-associated disorders remain unknown.<sup>1</sup> A variety of anatomical structures including the facet joint, the intervertebral disc, the anterior longitudinal ligament, the vertebral artery, the paraspinal muscles, the dorsal root ganglion, and components of the central nervous system have been identified as potential injury sites without the necessary supporting clinical or biomechanical evidence.<sup>2,4-8</sup> Establishing the specific anatomic injury sites and acceleration thresholds would allow for improved diagnosis, treatment and prevention of whiplash-associated disorders.





Clinical and pathological investigations have targeted the facet joints (FJs) as possible sources of pain in whiplash patients. The only clinical evidence comes from a series of studies that used nerve block and radiofrequency ablation of FJ afferents to successfully relieve pain.<sup>9-12</sup> Autopsy studies of subjects with soft-tissue neck injuries have revealed FJ hemarthroses, articular cartilage damage, synovial fold displacement, and capsular ligament (CL) tears.<sup>13,14</sup> In a whiplash simulation using cadavers, FJ diastases and CL tears were found in two of four specimens subjected to low-speed rear impacts.<sup>15</sup> Thus, sufficient clinical and pathological evidence exists to support the hypothesis of possible FJ injury during whiplash.

To explain the clinical observation of facet pain, two distinct FJ injury mechanisms have been hypothesized: excessive compression of the FJ articulation and CL strain beyond the physiologic limit. An *in vivo* study demonstrated that the C5-C6 intervertebral center of rotation was dynamically shifted superiorly during simulated whiplash impacts, implying that the facet articular surfaces were forcefully compressed during intervertebral extension.<sup>16</sup> Facet joint compression was also demonstrated directly in two cadaver studies, giving further support to the impingement injury mechanism hypothesis.<sup>17,18</sup> These investigators hypothesized that FJ compression could damage synovial folds that contain nociceptive nerve endings and potentially lead to facet pain.<sup>19,20</sup> Thus, both *in vivo* and *in vitro* work support the FJ compression injury mechanism hypothesis.

*In vitro* biomechanical studies have also identified excessive CL strain during whiplash as a potential injury mechanism. Two studies using quasi-static loading of cervical FJs to



simulate whiplash-type loading demonstrated that mean CL strains were below the subfailure thresholds, though isolated cases of CL strain in excess of the subfailure threshold were observed.<sup>21,22</sup> Direct measurement of CL elongation during simulated whiplash, using specialized transducers placed across the FJ in a whole cervical spine (WCS) model, showed maximum strains of less than 40% in a CL fiber.<sup>23</sup> During simulated whiplash of one cadaver, hypothetical CLs were constructed and tracked throughout the simulation, and a maximum strain of 51% at C5-C6 was reported.<sup>24</sup> While prior studies have evaluated the two FJ injury mechanism hypotheses separately, none have comprehensively analyzed complete cervical spine FJ kinematics at various impact accelerations.



## STATEMENT OF PURPOSE

We and other investigators have hypothesized that the facet joint is at risk of injury during whiplash. Two potential injury mechanisms have been proposed: excessive compression of the FJ articulation and CL strain beyond the physiologic limit. A biofidelic, whole-cervical spine model with muscle force replication has been developed to simulate whiplash. In order to develop a more thorough understanding of FJ injury mechanisms in whiplash, the goals of this study were to use this model to (1) quantify peak FJ compression, FJ sliding, and CL strain, (2) determine the acceleration thresholds at which these parameters exceed the physiologic levels, and (3) evaluate the two injury mechanisms hypotheses.



## MATERIALS AND METHODS

### *The Role of Various Investigators*

The work detailed in this dissertation represents a small portion of a multidisciplinary biomechanical study of whiplash. Dr. Panjabi was responsible for the overall conception, design and direction of the investigation. Mr. Ivancic and others worked on the development of the current in vitro model and methods of data analysis. Mr. Ivancic and Dr. Ito performed the actual whiplash simulation. The author's role was primarily in the design of the facet joint and capsular ligament model, design of the method to evaluate the soft-tissues throughout the whiplash simulation, data analysis and interpretation of the data.

### *Specimen Preparation and Radiography*

*WCS Preparation for Intact Flexibility Testing.* Six fresh-frozen human cadaveric osteoligamentous WCS specimens (C0-T1) were mounted in resin (Fiberglass Evercoats, Cincinnati, OH) at the occiput and T1 according to a pre-defined neutral posture.<sup>25</sup> To attach the lightweight motion-tracking flags, a headless wood screw was drilled into the anterior aspect of each vertebra (C1-C7). The flags consisted of 3 mm diameter hollow brass tubes with two white, spherical, radio-opaque markers (**Figure 1**). A flag was fitted rigidly onto each wood screw, and additional flags were attached to the occipital and T1 mounts.

*Radiography and Facet Geometry.* A lateral x-ray of the WCS in the neutral posture was taken and digitally scanned (Adobe Photoshop version 6.01, San Jose, CA). The FJs of each functional spinal unit (FSU), C2-C3 to C6-C7, were identified on the radiographs,





and three pairs of points were selected to define the articular surfaces (**Figure 1**). The origins and insertions of three CL fibers were also selected. The length and spacing of the three CL fibers were proportional to the size of each FJ, such that the average CL dimensions were equal to the average human CL (8.74 mm long and 7.15 mm wide).<sup>26</sup> The points of interest on the radiograph were digitized to define geometrical rigid body relationships between the centers of the flag markers and the facet points on each vertebra.

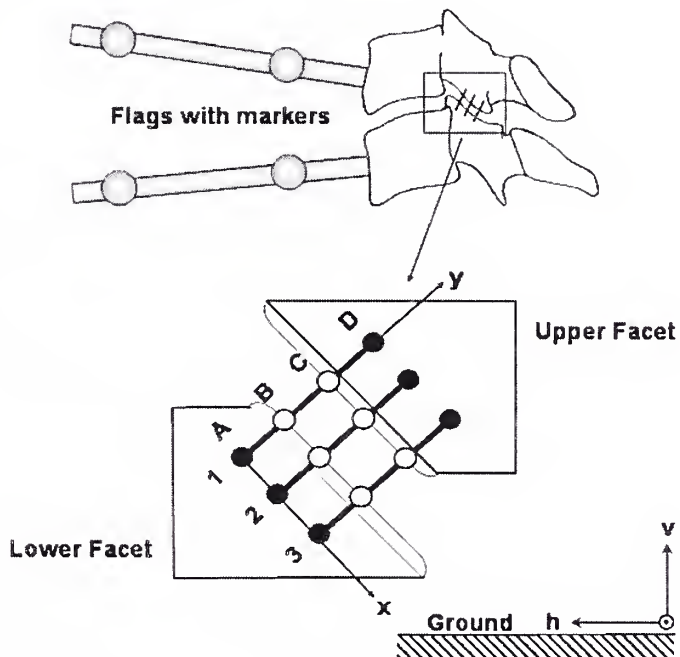


**Figure 1.** Schematic showing functional spinal unit with motion-tracking flags and facet points. The articular surfaces were defined by points B and C, and the capsular ligaments were defined by points A and D. The ground coordinate system h-v was fixed to the ground, and the FJ coordinate system x-y was fixed to the lower facet and moved with it.



*WCS+MFR Preparation for Whiplash Simulation.* To prepare a specimen for whiplash simulation, a surrogate head (mass 3.3 kg and sagittal plane moment of inertia 0.035 kg m<sup>2</sup>) was rigidly attached to the occipital mount via two bolts. The surrogate head and spine were stabilized using the compressive muscle force replication (MFR) system (**Figure 2**).<sup>27</sup> The MFR system consisted of four anterior, two posterior and eight lateral cables attached to pre-loaded springs anchored to the base. The stiffness coefficient of each spring was 4.0 N/mm. The anterior cables ran through guideposts at C4 (two cables per post), through pulleys within the T1 mount and finally were connected to two springs (two cables per spring). The preload in each anterior spring was 15 N. Two posterior MFR cables were connected to the occipital mount and ran through wire loops attached to the spinous processes of each vertebra (C2 to C7), through a pulley within the T1 mount and to a spring preloaded at 30 N. Bilateral MFR cables originated from C0, C2, C4 and C6, passed alternately along lateral guide rods, ran through pulleys at the T1 mount and were attached to the springs preloaded at 30 N. With this MFR arrangement the compressive pre-loads at each intervertebral level were: 120 N (C0-C1, C1-C2); 180 N (C2-C3, C3-C4); 240 N (C4-C5, C5-C6); and 300 N (C6-C7, C7-T1). The MFR system fully supported the head such that no counterweight was needed to suspend the head in the neutral posture. A C0-C2 flexion limiter was used to simulate the effect of contact between the chin and the anterior cervical structures (i.e. skin, subcutaneous fat, strap muscles, sternum) on flexion of C0-C1 and C1-C2.<sup>28</sup> It consisted of a nylon-coated steel cable (180 N load capacity, 0.6 mm diameter, part no. Y-MCX-24, Small Parts, Inc., Miami Lakes, FL) secured to the occipital mount and to the C2 spinous process and allowed approximately 30° of sagittal rotation, consistent with the in vivo data of the



normal cervical spine.<sup>29-31</sup> This constituted the WCS+MFR model. A C0-C2 flexion limiter was used to allow only physiologic flexion of C0-C1 and C1-C2.

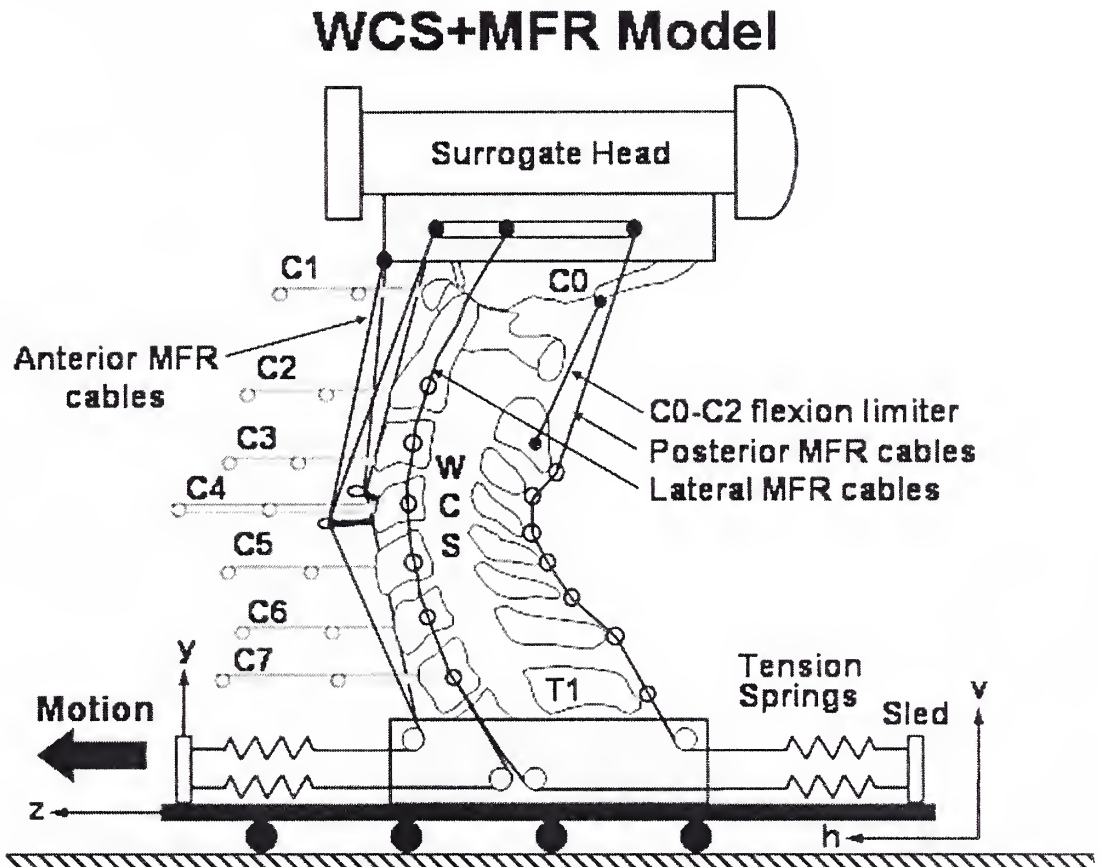


**Figure 2.** Schematic demonstrating the whole cervical spine model with muscle force replication system.

### *Physiologic FJ Displacements and CL Strains*

Intact WCSs underwent standard flexibility testing to determine physiologic FJ displacements and CL strains (**Figure 3**).<sup>32</sup> Pure flexion and extension moments up to a maximum of 1.5 Nm were applied to the occipital mount in four equal steps. Physiologic FJ displacements and CL strains were defined as the peak values obtained during the flexibility testing and were calculated using the method described below.



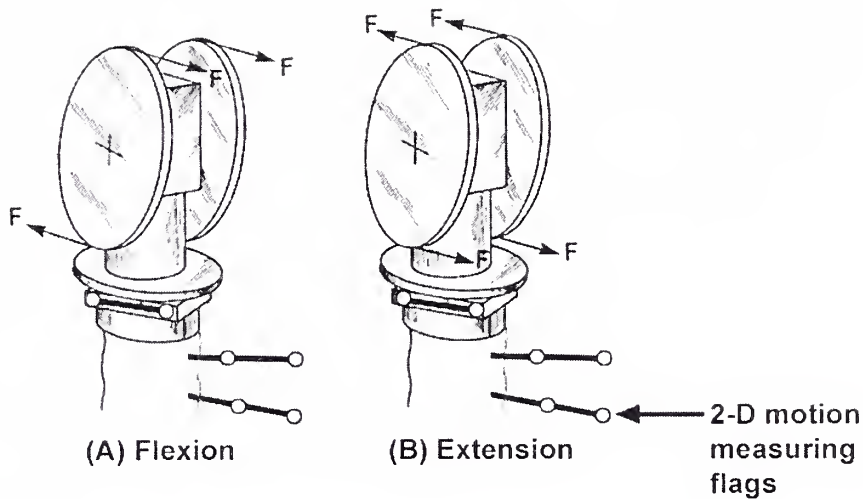


**Figure 3.** Schematic representation of sagittal plane flexibility testing.

### *Whiplash Simulation and Monitoring*

Rear-impact whiplash simulation was performed using a previously developed bench-top sled apparatus.<sup>27,33</sup> Incremental trauma protocol was used to rear-impact the WCS+MFR specimens at maximum horizontal T1 accelerations of 3.5, 5, 6.5 and 8 g, in addition to an initial 2 g simulation that served as the dynamic pre-conditioning. High-speed digital cameras (Fastcam, Super 10K, model PS-110, Eastman Kodak Co, Rochester, NY) recorded the spinal motions at 500 f/s.

### *FJ Displacements and CL Strains During Whiplash*

The previously described geometrical rigid body relationships between the flag markers and facet points established on the x-ray were used to superimpose the points onto the first frame of the high-speed movie. Custom motion-tracking software, written in Matlab (The Mathworks Inc., Natick, MA, USA), computed the vertebral body rotations and flag marker translations at each subsequent frame in the ground coordinate system h-v (**Figure 1**). These data, together with the geometrical rigid body relationships, were used to calculate the translation of each facet point in the ground coordinate system h-v.





Translations of the upper facet points relative to the lower facet points were determined in the local FJ coordinate system x-y (**Figure 1**). The FJ coordinate system was fixed to the lower facet and moved with it. Its origin was at A1, the positive x-axis pointed towards A3, and the positive y-axis was orthogonal to the x-axis and pointed towards D1 in the neutral posture. Translation of the upper facet relative to the lower was defined as either: posterior FJ sliding (positive x-axis direction), anterior FJ sliding (negative x-axis direction), FJ separation (positive y-axis direction), or FJ compression (negative y-axis direction). The strains within the three CL fibers spanning each FJ were also determined.

### ***Error Analysis***

A custom jig was constructed to determine the overall translation error, which included errors associated with the measurement system, the custom motion tracking software and the computation of CL strains and FJ displacements (**Figure 4**). The jig consisted of two motion-tracking flags with three markers per flag (flag 1: markers 1A, 1B and 1C; flag 2: markers 2A, 2B and 2C). The flags were connected by a hinge joint, and the marker 1C remained fixed. The marker 2C was translated horizontally using an automated digital micrometer (resolution 0.0001 mm, Oriel Corporation, Stamford, CT) in 50 increments of 0.1 mm each, and a digital image was recorded at each motion step. The custom software was used to track the positions of markers 1A, 1B, 2A and 2B in the ground coordinate system h-v. Using these data, the translation of marker 2C relative to 1C was calculated. The average translation error was 0.3 mm (SD 0.2 mm).



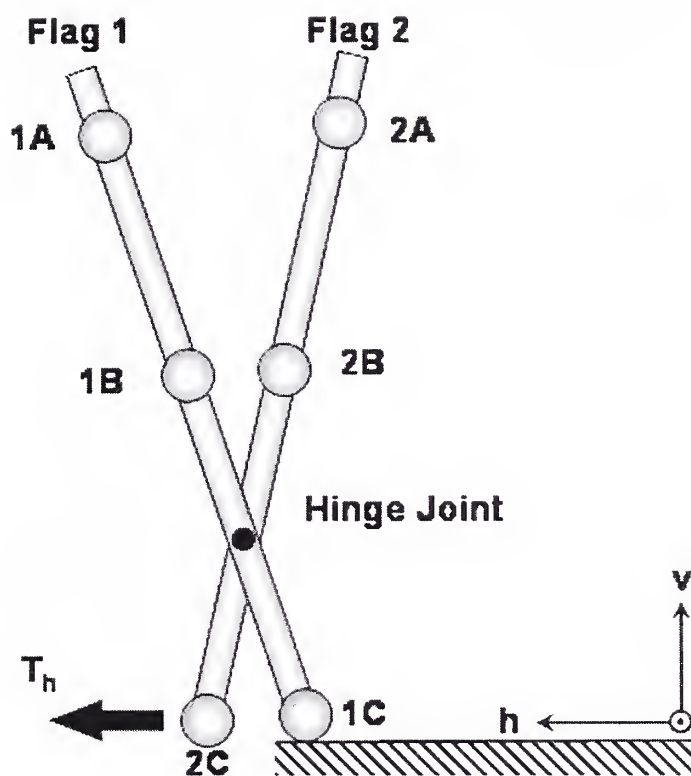


**Figure 4.** Schematic of the jig used to determine the system error associated with computation of kinematic data. The jig consisted of two motion-tracking flags with three markers per flag (flag 1: markers 1A, 1B and 1C; flag 2: markers 2A, 2B and 2C). The flags were connected by a hinge joint, and marker 1C remained fixed. Horizontal translation ( $T_h$ ) was applied to marker 2C using a digital micrometer in 50 equal steps and a digital image was recorded at each motion step.

#### *Data Analyses*

FJ compression, FJ sliding and CL strain data were low pass digitally filtered at a cut-off frequency of 30 Hz. For each whiplash simulation, the peak FJ compression, posterior FJ



sliding and CL strain were determined for each intervertebral level (C2-C3 to C6-C7) during the total intervertebral extension time period. The time at which the peak FJ compression, FJ sliding and CL strain occurred was expressed as percentages of the total intervertebral extension time period so that data from different impacts could be combined.

Single factor, repeated measures ANOVA ( $p < 0.05$ ) and Bonferroni post-hoc tests (Minitab Rel. 13, State College, PA) were used to compare peak FJ compression, posterior FJ sliding and CL strain during the whiplash simulation with corresponding physiologic values determined from the flexibility testing. Pairwise comparisons among times of peak FJ compression, posterior FJ sliding, CL strain and intervertebral extension were made in order to determine the temporal event patterns.



## RESULTS

### *Representative Example*

Kinematic data varied among specimens and intervertebral levels, however a general pattern emerged as demonstrated by the C6-C7 facet joint of human specimen #2 during the 5 g simulation (**Figure 5**).

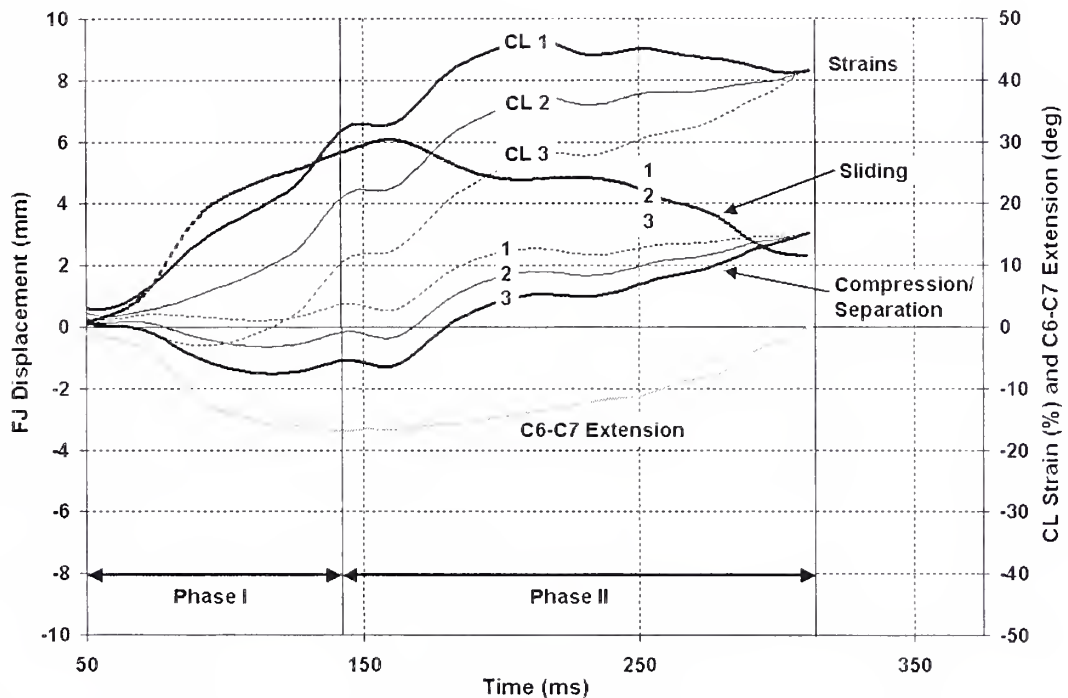


**Figure 5.** Facet joint (FJ) displacements and capsular ligament (CL) strains during simulated whiplash (specimen #2 during 5 g simulation). Compression (negative) and separation (positive) are shown for the anterior (1), middle (2), and posterior (3) articular surface points. Sliding (posterior positive, anterior negative) is shown only for the mid articular surface point (2) as differences in sliding among the three articular surface points were negligible. Strains are shown for the anterior (CL 1), middle (CL 2) and posterior (CL 3) CL fibers.





Two distinct phases were observed, based on intervertebral rotation. Phase I began with the onset of extension from the neutral posture and ended at peak intervertebral extension, while Phase II spanned from the peak intervertebral extension to return to the neutral posture. As C6 extended relative to C7 in Phase I, the upper facet slid posteriorly along the lower facet, and the posterior region compressed with a peak velocity of 54.6 mm/s. The CL strains tended to increase during Phase I, with the greatest CL strain occurring in the anterior fiber and the least in the posterior fiber. During Phase II, the relative motion of the upper facet was reversed as it began to slide anteriorly and separate from the lower facet. Capsular ligament strains continued to increase, and the maximum CL strain was observed in the anterior fiber in the middle of Phase II. The peak rate of CL elongation was 47.3 mm/s.

### *Six Specimens*

Maximum FJ compression occurred in the posterior region of the facet joint, while maximum CL strain was achieved in the anterior CL fiber. The differences in FJ sliding among the three pairs of articular surface points were negligible, hence peak FJ sliding at the mid articular surface was chosen for further analyses. Facet joint compression above the physiologic level was first observed at C4-C5 during the 3.5 g simulation (**Figure 6**). Non-physiologic compression was also observed at C2-C3 during the 6.5 g and 8 g simulations. FJ compression reached a maximum of 2.6 mm at C4-C5 during the 5 g simulation, and compressions did not consistently increase at accelerations above 5 g (**Table 1**). Peak posterior FJ sliding tended to increase with impact severity and was greatest in the lower cervical spine region (**Figure 7**). Significant increases first occurred at C4-C5 and C5-C6 during the 5 g simulation and spread to adjacent levels with



increasing acceleration. Maximum FJ sliding was 5.4 mm and occurred at C6-C7 during the 8 g simulation (Table 2).

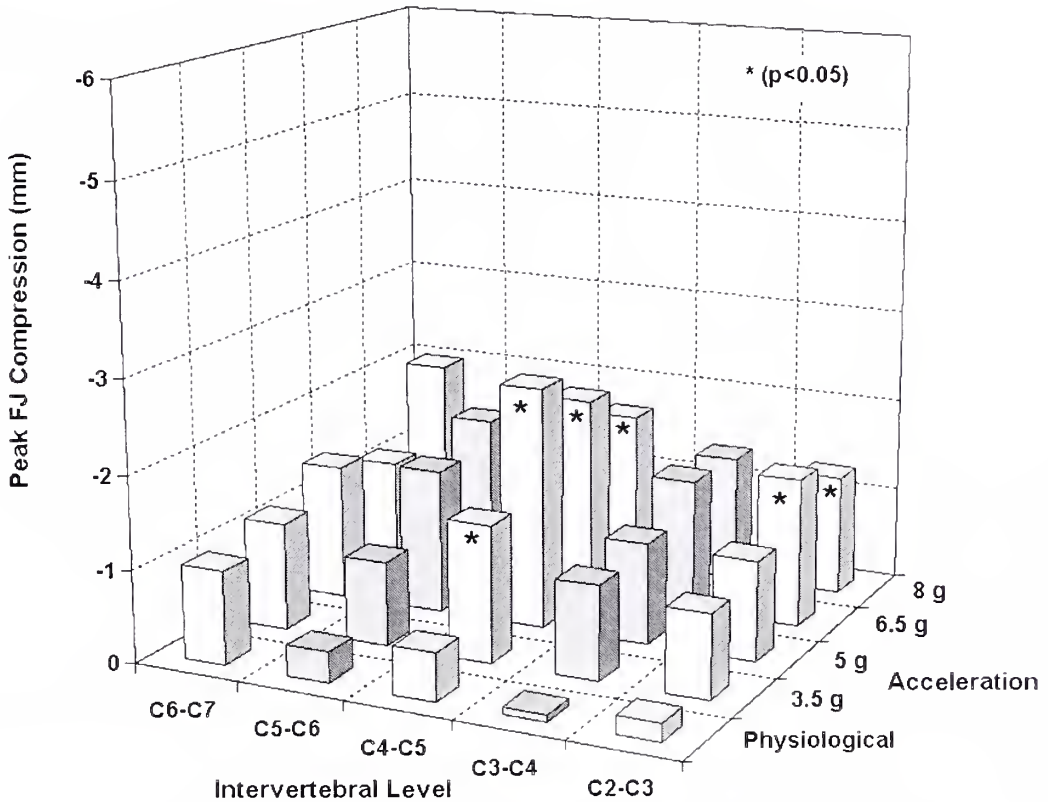


**Figure 6.** Average peak facet joint (FJ) compression at C2-C3 to C6-C7 during physiologic loading and simulated whiplash.

In general, the peak CL strains were highest in the lower cervical spine and increased with acceleration (Figure 8). Significant increases ( $p < 0.05$ ) over the physiologic strains occurred first during the 6.5 g simulation at C3-C4 and were also observed at C6-C7 during the 8 g simulation. At 8 g, CL strains ranged from 16.7% at C2-C3 to 39.9% at C6-C7 (Table 3). At 5 g and above, CL strains in the lower cervical spine fell into the



subfailure injury range (35.0%-64.6%) but were well below the failure threshold (94.0%-103.6%) as defined by prior studies.<sup>21,22</sup>

**Table 1.** Average (SD) peak facet joint (FJ) compression (mm) during simulated whiplash and comparisons to physiologic FJ compression (mm).

	<b>C2-C3</b>	<b>C3-C4</b>	<b>C4-C5</b>	<b>C5-C6</b>	<b>C6-C7</b>
<b>Physiologic</b>	-0.2 (0.2)	-0.1 (0.1)	-0.5 (0.5)	-0.3 (0.3)	-1.0 (0.8)
<b>3.5 g</b>	-0.9 (0.3)	-1.0 (1.4)	-1.5 (1.7)	-0.9 (0.6)	-1.2 (0.9)
<b>p-value</b>	0.2831	0.8074	0.0469	1.0000	1.0000
<b>5 g</b>	-1.1 (0.5)	-1.1 (0.6)	-2.6 (1.9)	-1.5 (2.1)	-1.4 (1.6)
<b>p-value</b>	0.1378	0.7363	0.0002	0.3413	0.8208
<b>6.5 g</b>	-1.6 (1.4)	-1.4 (1.4)	-2.2 (1.4)	-1.8 (2.0)	-1.2 (1.4)
<b>p-value</b>	0.0067	0.2541	0.0015	0.1698	1.0000
<b>8 g</b>	-1.3 (0.7)	-1.4 (1.1)	-1.7 (1.5)	-1.7 (1.3)	-2.0 (1.5)
<b>p-value</b>	0.0379	0.3151	0.0083	0.2003	0.3409



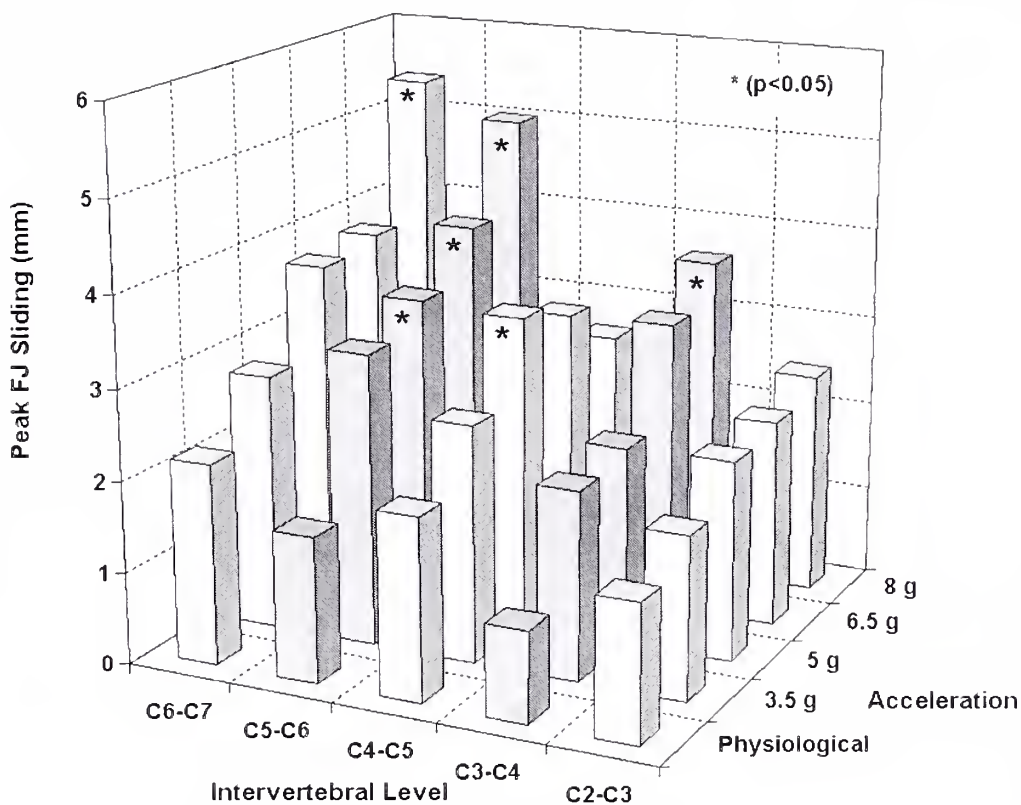


**Figure 7.** Average peak facet joint (FJ) sliding at C2-C3 to C6-C7 during physiologic loading and simulated whiplash.

Since the lower cervical spine demonstrated the most consistent and dramatic kinematic changes, the average times of peak FJ compression, FJ sliding and CL strain were analyzed for C5-C6 and C6-C7 for all accelerations (**Table 4**). On average, peak FJ compression occurred first, followed by peak FJ sliding and then peak CL strain. Peak FJ sliding occurred early in Phase II, peak CL strain occurred in the middle of Phase II, while the time of peak FJ compression could not be differentiated from the peak intervertebral extension.





**Table 2.** Average (SD) peak facet joint (FJ) sliding (mm) during simulated whiplash and comparisons to physiologic FJ sliding (mm).

	<b>C2-C3</b>	<b>C3-C4</b>	<b>C4-C5</b>	<b>C5-C6</b>	<b>C6-C7</b>
<b>Physiologic</b>	1.5 (0.9)	1.0 (0.6)	2.0 (0.8)	1.6 (1.1)	2.2 (0.7)
<b>3.5 g</b>	1.8 (1.0)	2.1 (1.5)	2.6 (2.4)	3.2 (1.3)	2.8 (1.7)
<b>p-value</b>	1.0000	1.0000	0.9198	0.1123	1.0000
<b>5 g</b>	2.2 (1.4)	2.2 (2.0)	3.4 (2.1)	3.5 (1.4)	3.7 (1.7)
<b>p-value</b>	0.6542	1.0000	0.0363	0.0435	0.2319
<b>6.5 g</b>	2.3 (1.9)	3.2 (2.9)	3.2 (2.0)	4.0 (1.3)	3.8 (1.7)
<b>p-value</b>	0.5123	0.1146	0.1092	0.0073	0.1747
<b>8 g</b>	2.5 (1.7)	3.6 (3.5)	2.6 (2.1)	5.0 (2.4)	5.4 (2.3)
<b>p-value</b>	0.2486	0.0491	0.7894	0.0002	0.0025



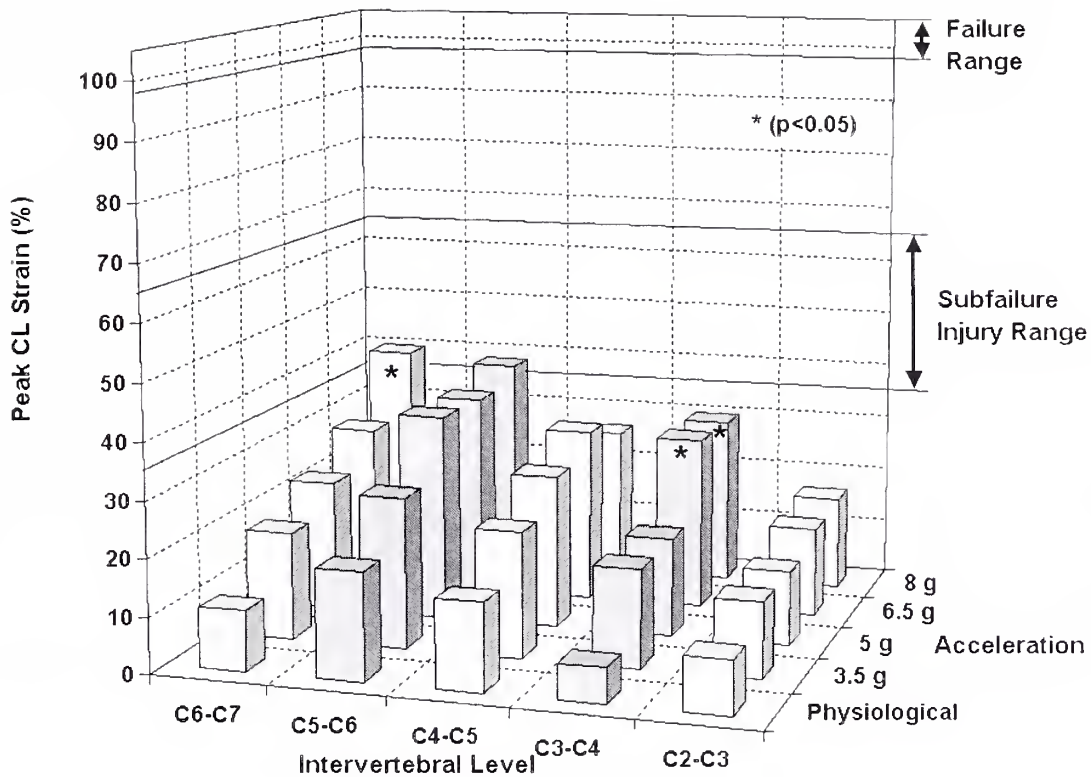


**Figure 8.** Average peak capsular ligament (CL) strains at C2-C3 to C6-C7 during physiologic loading and simulated whiplash. Subfailure injury and failure ranges are from Winkelstein et al. 2000<sup>21</sup> and Siegmund et al. 2001<sup>22</sup>.



**Table 3.** Average (SD) peak capsular ligament (CL) strains (%) during simulated whiplash and comparisons to physiologic CL strains (%).

	<b>C2-C3</b>	<b>C3-C4</b>	<b>C4-C5</b>	<b>C5-C6</b>	<b>C6-C7</b>
<b>Physiologic</b>	9.4 (7.1)	6.2 (7.9)	15.4 (10.9)	19.0 (17.9)	10.7 (9.3)
<b>3.5 g</b>	13.4 (9.3)	17.4 (15.2)	22.3 (20.6)	26.8 (17.9)	18.9 (14.2)
<b>p-value</b>	1.0000	0.6033	0.8602	1.0000	1.0000
<b>5 g</b>	13.2 (8.1)	17.6 (14.7)	27.3 (24.5)	36.8 (25.9)	23.3 (14.5)
<b>p-value</b>	1.0000	0.5738	0.2573	0.4376	0.6589
<b>6.5 g</b>	15.8 (13.5)	30.8 (25.1)	31.1 (22.5)	35.9 (21.9)	28.8 (20.0)
<b>p-value</b>	0.6939	0.0148	0.0883	0.5081	0.2068
<b>8 g</b>	16.7 (6.3)	29.9 (17.8)	26.5 (18.7)	38.5 (24.6)	39.9 (26.3)
<b>p-value</b>	0.5021	0.0191	0.3116	0.3252	0.0132



**Table 4.** Average times of key events in whiplash at C5-C6 and C6-C7.

Average (SD) times (%) normalized to total intervertebral extension time period.

Significant pairwise comparisons ( $p < 0.05$ ) among times of events are indicated with brackets.

Event	Time
Peak FJ Compression	43.3 (20.0)
Peak Intervertebral Extension	48.3 (13.4)
Peak FJ Sliding	59.7 (25.2)
Peak CL Strain	71.2 (22.6)





## DISCUSSION

While prior studies have evaluated facet joint (FJ) kinematics and capsular ligament (CL) strain during simulated whiplash separately<sup>17,18,23,24</sup>, no single study has comprehensively analyzed FJ compression, FJ sliding and CL strain throughout the entire cervical spine at multiple impact accelerations. In the current whiplash simulation, the posterior region of the FJ was compressed, and the upper facet slid posteriorly along the lower facet during intervertebral extension (Phase I)(**Figure 9**). Facet joint compression exceeded physiologic levels at C2-C3 and C4-C5, reaching a maximum of 2.6 mm at C4-C5 during the 5 g simulation. The FJ compression was most likely due to synovial fold compression, articular cartilage deformation on both facet surfaces, and elastic deformations of the neural arches. After motion of the upper facet reversed (Phase II), peak CL strain occurred due to the separation of the facets while the upper facet remained posterior to the lower facet. Thus, both FJ sliding and FJ separation contributed to peak CL strain. Facet joint compression exceeded physiologic levels at 3.5 g and above, suggesting that compression injury may occur at low impact accelerations. Capsular ligament strain exceeded the physiologic values at 6.5 g and above, validating it as a potential injury mechanism as well.

The limitations of the current whole cervical spine model with muscle force replication (WCS+MFR) must be considered when formulating conclusions regarding clinically relevant injury mechanisms. These limitations, including the fixation of T1 to the trauma sled and the lack of active muscle force simulation, have been previously discussed.<sup>27,33</sup> Due to the scarcity of human cadaveric material, many previous in vitro whiplash



simulations have been performed using between one and four specimens.<sup>17,18,24,34,35</sup> In the current study, six specimens were used. Despite the variability among the specimens, statistically significant increases over physiologic FJ compression and sliding and CL strain were observed. The calculation of FJ kinematics was based on the assumption that the vertebra and motion-tracking flag constituted a rigid body. During whiplash simulation it was unlikely that vertebral deformation was of a sufficient magnitude to significantly alter the results. The CL fibers analyzed in this study were constructed based on the size of the individual facet joints and the dimensions of the average human CL.<sup>26</sup> As such, they were approximate representations of the actual ligaments. Despite these limitations, we believe our results are clinically relevant.

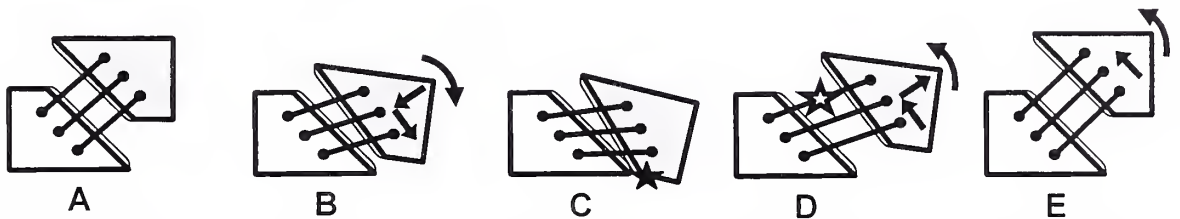


**Figure 9.** General facet joint (FJ) kinematics throughout intervertebral extension during whiplash. **A**, In the neutral position, capsular ligament (CL) fibers are perpendicular to the FJ and have no strain. **B**, In the middle of Phase I, the upper facet slid posterior relative the lower facet and the posterior region of the FJ was compressed. **C**, At peak intervertebral extension (end of Phase I), peak FJ compression occurred. Peak FJ sliding occurred shortly thereafter. **D**, In the middle of Phase II, peak CL strain occurred in the anterior CL fiber as the facets separated while the upper facet was still posterior to its neutral position. **E**, At the end of Phase II, the CL fibers were again perpendicular to the FJ though strained due to separation of the facets.



Our data support the findings of previous *in vivo* and *in vitro* studies. Kaneoka et al performed an *in vivo* whiplash study that demonstrated that the C5-C6 center of rotation was shifted superiorly in four of ten subjects during whiplash simulation and hypothesized that FJ impingement could injure the synovial fold.<sup>16</sup> Their results provided implicit evidence of FJ compression, and the results of the current study confirmed this hypothesis. In an *in vitro* study that evaluated FJ compression in the lower spine during whiplash simulation, Cusick et al reported 1.0 mm of compression at the posterior region of the FJ at an acceleration level of 4 g.<sup>17</sup> Using the same experimental methods, Yoganandan et al reported 2.8 mm of FJ compression at C5-C6 during a 4.4 g simulation.<sup>18</sup> These data compare favorably to the compression observed at 5 g in the lower spine in the current study, which ranged from 1.4 mm at C6-C7 to 2.6 mm at C4-C5. While these prior studies have focused on FJ compression in the lower spine, the current study demonstrated that FJ compression in excess of physiologic levels occurred in the upper cervical spine as well.

Facet joint compression that exceeds physiologic levels could potentially injure the facet articular cartilage. Prior animal studies have demonstrated that acute loading of the patellofemoral joint using loads above physiologic levels but below the fracture threshold can lead to osteoarthritic changes in the cartilage.<sup>36-38</sup> If the upper facet collided with the lower facet with sufficient force to cause irreversible damage to the cartilage matrix or chondrocytes, this could result in cartilage degeneration and osteoarthritis. However, the injury threshold of facet cartilage is unknown, and this study was limited to kinematic



analysis of the FJ. As such, we cannot make conclusions about the magnitude of facet loading during whiplash and can only suggest that cartilage injury is a possibility.

Other authors have suggested that the synovial fold is at risk for injury during FJ compression, and the current study supports this hypothesis.<sup>16,17,20</sup> Synovial folds are present in most FJs, and 75% of synovial folds have a component located in the posterior region of the joint.<sup>19</sup> It is this portion of the synovial fold that would be at greatest risk due to the FJ compression. Since the synovial fold contains neurovascular structures, injury would likely result in pain and inflammation.<sup>20</sup>

Capsular ligament strains in the subfailure injury range were observed in the current study, suggesting that CL injury was possible. The only data available for CL subfailure thresholds were obtained measuring maximum principal strains under static loading, so comparisons to these data must be made cautiously.<sup>21,22</sup> Nonetheless, if subfailure injury were to occur, this could result in increased CL laxity. The CL contains both mechanoreceptive and nociceptive nerve endings, and the facet capsule is lined with synovium.<sup>39</sup> Excessive CL strain could potentially injure these structures and generate pain.

This study has identified facet articular cartilage, the synovial fold and the facet capsule as structures at risk for injury during whiplash due to excessive FJ compression or CL strain. Injury to the articular cartilage, synovial fold, or CL would likely result in inflammation, which could potentially sensitize peripheral and central nociceptive





neurons.<sup>40,41</sup> This sensitization process could lead to the lowering of nociceptive firing thresholds, resulting in pain during normal motion. Mechanoreceptors in the facet capsule or synovial fold could also be damaged during whiplash. Animal experiments have suggested that similar mechanoreceptors in lumbar facet capsules play a role in proprioception.<sup>42,43</sup> Disruption of the transmission of proprioceptive information could lead to dysfunction of the spinal stabilizing system and the potential for spinal instability or uncoordinated, painful muscle contraction.<sup>44-46</sup> While the details of these hypothetical pain pathways remain unknown, it is reasonable to assume that excessive FJ compression or CL strain could lead to the chronic symptoms associated with whiplash injury.



## REFERENCES

1. Spitzer WO, Skovron ML, Salmi LR, et al. Scientific monograph of the Quebec Task Force on Whiplash-Associated Disorders: redefining "whiplash" and its management. *Spine* 1995;20:1S-73S.
2. Barnsley L, Lord S, Bogduk N. Whiplash injury. *Pain* 1994;58:283-307.
3. Richter M, Otte D, Pohlemann T, et al. Whiplash-type neck distortion in restrained car drivers: frequency, causes and long-term results. *Eur Spine J* 2000;9:109-17.
4. Nibu K, Cholewicki J, Panjabi MM, et al. Dynamic elongation of the vertebral artery during an in vitro whiplash simulation. *Eur Spine J* 1997;6:286-9.
5. Ommaya AK, Faas F, Yarnell P. Whiplash injury and brain damage: an experimental study. *Jama* 1968;204:285-9.
6. Ortengren T, Hansson HA, Lovsund P, et al. Membrane leakage in spinal ganglion nerve cells induced by experimental whiplash extension motion: a study in pigs. *J Neurotrauma* 1996;13:171-80.
7. Nederhand MJ, Hermens HJ, MJ IJ, et al. Chronic neck pain disability due to an acute whiplash injury. *Pain* 2003;102:63-71.
8. Panjabi MM, Cholewicki J, Nibu K, et al. Mechanism of whiplash injury. *Clin Biomech* 1998;13:239-49.
9. Barnsley L, Lord S, Bogduk N. Comparative local anaesthetic blocks in the diagnosis of cervical zygapophysial joint pain. *Pain* 1993;55:99-106.
10. Barnsley L, Lord SM, Wallis BJ, et al. The prevalence of chronic cervical zygapophysial joint pain after whiplash. *Spine* 1995;20:20-5; discussion 6.
11. Lord SM, Barnsley L, Wallis BJ, et al. Chronic cervical zygapophysial joint pain after whiplash. A placebo-controlled prevalence study. *Spine* 1996;21:1737-44; discussion 44-5.
12. Lord SM, Barnsley L, Wallis BJ, et al. Percutaneous radio-frequency neurotomy for chronic cervical zygapophyseal-joint pain. *N Engl J Med* 1996;335:1721-6.
13. Jonsson H, Jr., Bring G, Rauschnig W, et al. Hidden cervical spine injuries in traffic accident victims with skull fractures. *J Spinal Disord* 1991;4:251-63.
14. Taylor JR, Twomey LT. Acute injuries to cervical joints. An autopsy study of neck sprain. *Spine* 1993;18:1115-22.



15. Yoganandan N, Cusick JF, Pintar FA, et al. Whiplash injury determination with conventional spine imaging and cryomicrotomy. *Spine* 2001;26:2443-8.
16. Kaneoka K, Ono K, Inami S, et al. Motion analysis of cervical vertebrae during whiplash loading. *Spine* 1999;24:763-9.
17. Cusick JF, Pintar FA, Yoganandan N. Whiplash syndrome: kinematic factors influencing pain patterns. *Spine* 2001;26:1252-8.
18. Yoganandan N, Pintar FA, Cusick JF. Biomechanical analyses of whiplash injuries using an experimental model. *Accid Anal Prev* 2002;34:663-71.
19. Inami S, Kaneoka K, Hayashi K, et al. Types of synovial fold in the cervical facet joint. *J Orthop Sci* 2000;5:475-80.
20. Inami S, Shiga T, Tsujino A, et al. Immunohistochemical demonstration of nerve fibers in the synovial fold of the human cervical facet joint. *J Orthop Res* 2001;19:593-6.
21. Winkelstein BA, Nightingale RW, Richardson WJ, et al. The cervical facet capsule and its role in whiplash injury: a biomechanical investigation. *Spine* 2000;25:1238-46.
22. Siegmund GP, Myers BS, Davis MB, et al. Mechanical evidence of cervical facet capsule injury during whiplash: a cadaveric study using combined shear, compression, and extension loading. *Spine* 2001;26:2095-101.
23. Panjabi MM, Cholewicki J, Nibu K, et al. Capsular ligament stretches during in vitro whiplash simulations. *J Spinal Disord* 1998;11:227-32.
24. Luan F, Yang KH, Deng B, et al. Qualitative analysis of neck kinematics during low-speed rear-end impact. *Clin Biomech (Bristol, Avon)* 2000;15:649-57.
25. Braakman R, Penning L. Injuries of the cervical spine. Netherlands: Excelptra Media, 1971.
26. Panjabi MM, Oxland TR, Parks EH. Quantitative anatomy of cervical spine ligaments. Part II. Middle and lower cervical spine. *J Spinal Disord* 1991;4:277-85.
27. Ivancic PC, Panjabi M, Ito S, et al. A biofidelic osteoligamentous cervical spine model with muscle force replication for whiplash trauma simulation. Proceedings of the Cervical Spine Research Society. Miami, FL, 2002:180-2.
28. Panjabi MM, Miura T, Cripton PA, et al. Development of a system for in vitro neck muscle force replication in whole cervical spine experiments. *Spine* 2001;26:2214-9.
29. Dvorak J, Panjabi MM, Novotny JE, et al. In vivo flexion/extension of the normal cervical spine. *J Orthop Res* 1991;9:828-34.



30. Lind B, Sahlbom H, Nordwall A, et al. Normal range of motion of the cervical spine. *Arch Phys Med Rehabil* 1989;70:692-5.
31. Ordway NR, Seymour RJ, Donelson RG, et al. Cervical flexion, extension, protrusion, and retraction. A radiographic segmental analysis. *Spine* 1999;24:240-7.
32. Panjabi MM, Oxland TR, Lin RM, et al. Thoracolumbar burst fracture. A biomechanical investigation of its multidirectional flexibility. *Spine* 1994;19:578-85.
33. Panjabi MM, Cholewicki J, Nibu K, et al. Simulation of whiplash trauma using whole cervical spine specimens. *Spine* 1998;23:17-24.
34. Fast A, Sosner J, Begeman P, et al. Lumbar spinal strains associated with whiplash injury: a cadaveric study. *Am J Phys Med Rehabil* 2002;81:645-50.
35. Yoganandan N, Pintar FA, Klienberger M. Cervical spine vertebral and facet joint kinematics under whiplash. *J Biomech Eng* 1998;120:305-7.
36. Ewers BJ, Weaver BT, Sevensma ET, et al. Chronic changes in rabbit retro-patellar cartilage and subchondral bone after blunt impact loading of the patellofemoral joint. *J Orthop Res* 2002;20:545-50.
37. Triantafillopoulos IK, Papagelopoulos PJ, Politi PK, et al. Articular changes in experimentally induced patellar trauma. *Knee Surg Sports Traumatol Arthrosc* 2002;10:144-53.
38. Thompson RC, Jr., Oegema TR, Jr., Lewis JL, et al. Osteoarthrotic changes after acute transarticular load. An animal model. *J Bone Joint Surg Am* 1991;73:990-1001.
39. McLain RF. Mechanoreceptor endings in human cervical facet joints. *Spine* 1994;19:495-501.
40. Cavanaugh J. Neural mechanisms of idiopathic low back pain. In Weinstein JN GS ed. *Low Back Pain*. Rosemont: American Academy of Orthopaedic Surgeons, 1996:583-606.
41. Yaksh TL, Hua XY, Kalcheva I, et al. The spinal biology in humans and animals of pain states generated by persistent small afferent input. *Proc Natl Acad Sci U S A* 1999;96:7680-6.
42. Pickar JG, McLain RF. Responses of mechanosensitive afferents to manipulation of the lumbar facet in the cat. *Spine* 1995;20:2379-85.





43. Avramov AI, Cavanaugh JM, Ozaktay CA, et al. The effects of controlled mechanical loading on group-II, III, and IV afferent units from the lumbar facet joint and surrounding tissue. An in vitro study. *J Bone Joint Surg Am* 1992;74:1464-71.
44. Panjabi MM. The stabilizing system of the spine. Part I. Function, dysfunction, adaptation, and enhancement. *J Spinal Disord* 1992;5:383-9; discussion 97.
45. Holm S, Indahl A, Solomonow M. Sensorimotor control of the spine. *J Electromyogr Kinesiol* 2002;12:219-34.
46. Solomonow M, Zhou B, Baratta RV, et al. Neuromuscular disorders associated with static lumbar flexion: a feline model. *J Electromyogr Kinesiol* 2002;12:81-90.









**HARVEY CUSHING/JOHN HAY WHITNEY  
MEDICAL LIBRARY**

**MANUSCRIPT THESES**

Unpublished theses submitted for the Master's and Doctor's degrees and deposited in the Medical Library are to be used only with due regard to the rights of the authors. Bibliographical references may be noted, but passages must not be copied without permission of the authors, and without proper credit being given in subsequent written or published work.

This thesis by  
has been used by the following person, whose signatures attest their acceptance of the above restrictions.

---

---

**NAME AND ADDRESS**

**DATE**

YALE MEDICAL LIBRARY



3 9002 01065 7139



